Technological Impact of Hydromagnetic Micropolar Fluid Flow Over a Stretching Permeable Sheet with Thermal Radiation and Joule Heating Effects

E. O. Fatunmbi[1] and O. A. Sikiru[2]
[1 -2]Department of Mathematics and Statistics, Federal Polytechnic, Ilaro, Nigeria
E-mail: [1]olusojiephesus@yahoo.com, [2]olusegun.sikiru@federalpolyilaro.edu.ng
Corresponding author: olusojiephesus@yahoo.com

ABSTRACT
This present study focuses on the technological impact of hydromagnetic micropolar fluid flow and heat transfer over an inclined sheet with the effects of thermal radiation, Joule heating and non-uniform heat source/sink as well as surface mass flux. The governing equations of the flow and heat transfer have been reduced from partial to ordinary differential equations via similarity transformation. Subsequently, shooting techniques alongside fourth order Runge-Kutta integration scheme are employed to solved the transmuted equations. The influences of the main controlling parameters are analyzed using graphs and tables with appropriate discussion. The results compared favourably with the earlier reported data in the literature in the limiting cases. The results also showed that the skin friction coefficient can be reduced better by applying the non-Newtonian micropolar fluid and that the velocity as well as the temperature profiles accelerate with a rise in the radiation parameter.
Keywords: Micropolar fluid; thermal radiation; Joule heating; non-uniform heat source/sink

1.0 INTRODUCTION

Fluids are broadly classified as Newtonian or non-Newtonian, depending on their flow characteristics. Newtonian fluids are fluids in which the viscous stresses arising from its flow at every point, are linearly proportional to the local strain rate (Lukaszewic, 1999). These fluids obey Newton's law of viscosity. Examples are: water, kerosene, and alcohol. On the other hand, the non-Newtonian fluids are fluids which properties differ from those of Newtonian (classical) fluids, and thus fall outside the domain of the classical field theories. Most often, the viscosity of non-Newtonian fluids is dependent on shear rate or shear rate history. Examples of such fluids are ketchup, butter, cosmetics, polymer solutions, blood, colloids, mud flows, gels, biological fluids (mucus, semen, synovia fluid), cheese, etc.

In the recent times, the investigation of non-Newtonian fluids has been on the increase owing to its practical scientific, technological and industrial uses. Micropolar fluids belong to the class of non-Newtonian fluids due to its anti-symmetric stress tensor. The concept of micropolar fluids originated from Eringen (1966, 1972) as a sub-class of simple microfluid which was first introduced by Eringen (1964). Micropolar fluids consists of rigid, randomly oriented (or spherical) particles suspended in a viscous medium, where particles deformation is ignored. They are fluids with microstructure such that individual fluid particles may vary in shapes and rotate independently of the fluid rotation (Lukaszewicz, 1999).

Since introduction of the concept, it has become an active area of research for scientists and engineers because it offers a good mathematical model for examining the flow of complex and complicated fluids such as liquid crystals, polymeric fluids, suspension solution, fluids with certain additives, animal blood, fluids and clouds with dust (Chen et al., 2011; Mohamed and Abo-Dahab, 2009, Hayat *et al.*, 2011). Various applications in engineering and technology include polymer engineering, drug suspension in pharmacology, sediments in rivers, biological fluid modelling, crude oil extraction, food processing manufacturing and so on (Ariman *et al*., 1973).

The study of hydromagnetic fluid flow and heat transsfer over stretching sheet has become vital due to practical applications in industrial, technological and engineering operations. For instance, the extrusion of plastic sheet, metal extrusion, hot rolling, the extrusion of polymer sheet from a die, the cooling of metallic sheets, drawing of copper wires, glass blowing, textile and paper production, etc. It was Crane (1970) who pioneered such study. Also Gupta and Gupta (1977) extended the work of Crane to include heat transfer with suction or blowing. Several authors investigated such study (see Cortell, 2008; Kumar, 2009; Pal and Chatterjee, 2010; Mahmoud, 2011, Fatunmbi and Fenuga, 2018). In polymer extrusion for instance, during the fabrication processes, the material is made to enter into a cooling fluid after passing through a die, the quality of the final products depend, to some extent, on the kinematics of stretching and the rate of cooling during the fabrication processes. Thus, to obtain the quality desired, the rate of cooling can be controlled by the use of electrically conducting micropolar fluid.

Most transport phenomena both in nature and industies include flow of fluids driven by buoyancy forces due to variations in density as a result of temperature differences.. Hence, the application of magnetic field in engineering operations play a crucial in areas such as in plasma studies, nuclear reactors, oil exploration, geothermal energy extractions, MHD generators, and boundary layer control in the field of aerodynamic. To this end, various reaserchers have invesigated such studies. (see Sreenivasulu et al., 2018; Fatunmbi and Fenuga, 2018, Fatunmbi and Adeniyan, 2018, Kumar, 2009, etc).

In technology and engineering processes such as in the design of thrust bearing and radial diffusion and thermal oil recovery, etc. Suction/injection become important, for instance, iinjection can be applied in boundary layer control applications (e. g. film coating, polymer fiber coating and coating of wires), adding of reactants, prevention of corosion, reducing drag whereas suction can be applied to remove reactants in chemical processes (see Mukhopadhyay, 2013; Hayat *et al.* 2010).

Many of the engineering and manufacturing operations occur at high temperature. For instance, in nuclear power plants, gas turbines, space technology and various propulsion devices for aircraft (Ibrahim, 2014). Thus, the influence of thermal radiation on magnetohydrodynamic flow and heat transfer plays a key role for the design of relevant equipment. The quality of the end product obtained during fabrication processes depends on how well the heat can be controlled, hence, the desired product can be optimally achieved with the intended characteristics when there is accurate knowledge of radiation heat transfer. In view of these immense applications, studies involving thermal radiation have been widely investigated. Hamad *et al*. (2012) applied implicit finite difference method to numerically study the influence of thermal radiation on heat and mass transfer of Newtonian fluid with variable fluid properties. Darbhashayanam and Mendu (2014) examined thermal radiation and chemical reaction effects on MHD free convection heat and mass transfer in a micropolar fluid using Keller-box method. (see also Olanrewaju *et al.*, 2011; Fatunmbi and Adeniyan, 2018).

In view of the above discussions and technolgical applications, this study is set out to investigate numerically the technological impact of hydromagnetic micropolar fluid over an inclined permeable surface under the influence of thermal radiation, Joulean heating with variable electrical conductivity and magnetic field. Similarity transformation variables have been applied for the reduction of the modelled nonlinear partial differential equations governing the flow and heat transfer into a system of nonlinear ordinary differential equations and then solved via shooting techniques cum fourth order Runge-Kutta integration scheme.

2.0 The Development of the Problem

The flow is assumed to be two-dimensional, steady and electrically conducting, viscous and incompressible micropolar fluid over an inclined permeable sheet with thermal boundary condition taken to prescribed variable surface heat flux given as $-\kappa\frac{\partial T}{\partial y} = q_w = A\left(\frac{x}{L}\right)^n$, where A is a constant and n is power law temperature exponent parameter (see Figure 1). The flow direction is assumed to be in the x axis which is taken along the surface with y axis normal to it, the elcectrical conductivity varies with the fluid velocity in the direction of flow while the applied magnetic field varies in strength i.e. $\boldsymbol{B} = (0,\ B(x), 0)$.. The radiative heat flux along x axis is asummed to be neglible as compared to that of y direction. The magnetic Reynolds number is assumed to be sufficiently small such that the induced magnetic field is negligible in comparison to the applied magnetic field. Body forces such as Darcy, Forchheimer resistance are not considered in this study. Under the aforementioned assumptions as well as the Oberbeck-Boussinesq and the boundary layer approximations, the governing equations are given as.

$$\frac{\partial u}{\partial x} + \frac{\partial v}{\partial y} = 0 \tag{1}$$

$$u\frac{\partial u}{\partial x} + v\frac{\partial u}{\partial y} = \left(\nu + \frac{\mu_r}{\rho}\right)\frac{\partial^2 u}{\partial y^2} + \frac{\mu_r}{\rho}\frac{\partial N}{\partial y} + g\beta_T\,(T - T_\infty)cos\varphi - \frac{\sigma_0'(B(x))^{\,2}}{\rho}u, \tag{2}$$

$$\rho j\left(u\frac{\partial N}{\partial x} + v\frac{\partial N}{\partial y}\right) = \gamma\frac{\partial^2 N}{\partial y^2} - \mu_r\left(2N + \frac{\partial u}{\partial y}\right), \tag{3}$$

$$u\frac{\partial T}{\partial x}+v\frac{\partial T}{\partial y}=\frac{\kappa}{\rho cp}\left(1+\frac{16T_{\infty}^{3}\sigma^{\star}}{k^{\star}\kappa}\right)\frac{\partial^{2}T}{\partial y^{2}}+\frac{1}{\rho cp}(\mu+\mu_{r})\left(\frac{\partial u}{\partial y}\right)^{2}+\frac{\sigma_{0}'(B(x))^{2}}{\rho}u^{2}+\frac{q'''}{\rho cp}. \tag{4}$$

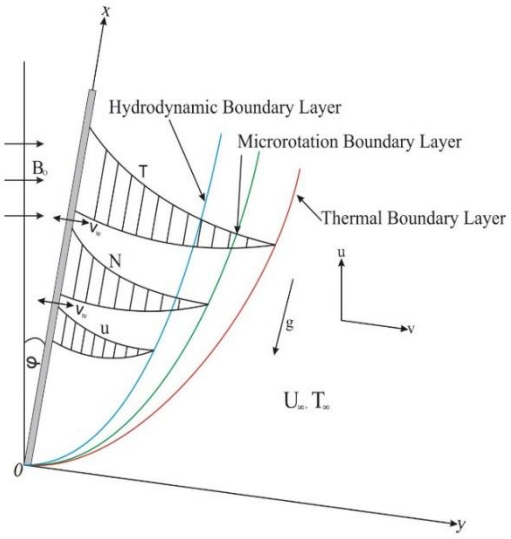

Figure. 1: Flow configuration and coordinate system

The boundary conditions are:

$$y=0:\ u=0,\ v=V_{w},\ N=-r\frac{\partial u}{\partial y}\ ,\ -\kappa\frac{\partial T}{\partial y}=q_{w}=A\left(\frac{x}{L}\right)^{n}\ , \tag{5}$$
$$y\to\infty:\ u=U_{\infty}=0,\ N=0,\ T\longrightarrow T_{\infty}.$$

In Eqs. (1-4), the velocity component in the direction of x and y are respectively denoted by u and v *while* ν is the coefficient of kinematic viscosity, T represents the fluid temperature whereas β_T is the thermal expansion coefficient, V_w *indicates the* suction/injection, g is the acceleration due to gravity, ρ is the density, c_{p} the specific heat at constant pressure, κ is the thermal conductivity, N is the component of microrotation normal to $xy-$ plane and γ is the spin gradient viscosity, φ stands for the inclination angle, μ symbolizes the dynamic viscosity, μ_r is the vortex viscosity. In Eq. (5), r is the microrotation boundary parameter having the interval $0\le r\le 1$. The case when $r=0$ represents the vanishing of the spin on the boundary as reporeted by Jena and Mathur (1981). When $r=1/2$, it depicts a weak concentration of micro-particles and the disapearance of anti-symmetric part of the stress tensor (Ahmadi, 1976). However, $r=1$ illustrates turbulent boundary layer flows as discussed by Peddieson (1972).
The electrical conductivity varies with the fluid velocity such as (see Helmy, 1995)

$$\sigma_{0}'=\sigma_{0}u, \tag{6}$$

while the applied magnetic field strength is a function of x such that

$$B(x)=B_{0}x^{-\frac{1}{2}}, \tag{7}$$

The symbol q′′′ in the energy equation (4) indicates the non-uniform heat source/sink and it is espressed as (see Rahman *et al*., 2009)

$$\mathrm{q}'''=\frac{\kappa}{2\nu x}\left[Q(T-T_{\infty})+Q^{*}(T_{w}-T_{\infty})\mathrm{e}^{-\eta}\right] \tag{8}$$

where $Q,\ Q^{\star}$ respectively represents the coefficient of space and temperature dependent heat source/sink. When $Q > 0\ and\ \ Q^{\star} > 0$ then, a case of heat source is implied, however, the a case of heat sink is indicated when $Q < 0\ and\ \ Q^{\star} < 0$.
The governing Eqs. (2-5) are transmuted ordinary differential equations by using Eq. (9)

$$\psi = (2\nu U_0 x)^{\frac{1}{2}} f(\eta),\ \ \eta = y\left(\frac{U_0}{2\nu x}\right)^{\frac{1}{2}},$$
$$N = \left(\frac{U_0^3}{2\nu L}\right)^{\frac{1}{2}} g(\eta),\ T = T_\infty + (T_w - T_\infty)\theta(\eta) \tag{9}$$

Substituting Eq. (9) into Eqs. (2-5) and taking cognizance of Eqs. (6-8) we obtained the following nonlinear coupled ordinary differential equations:

$$(1+K)f''' + ff'' + Kg' + Gr\theta cos\varphi - Mf'^{2} = 0 \tag{10}$$

$$\left(1+\frac{K}{2}\right)g'' + fg' + f'g - 2K(2g + f'') = 0 \tag{11}$$

$$(1+Rd)\theta'' + \Pr(f\theta' - (2n+1)f'\theta + Q\theta) + PrEc\, f''^{2} + PrEcMf'^{3} + (Q\theta + Q^{*}e^{-\eta}) = 0. \tag{12}$$

The corresponding boundary conditions are:

$$\eta = 0:\ f' = 0,\ f = fw,\ g = -rf'', \theta = -1,$$
$$\eta \longrightarrow \infty:\ f' = 0,\ g = 0,\ \theta = 0. \tag{13}$$

In Es. (10-13), the differentiation is done with respect to $\eta, K = \mu_r/\mu$ stands for the material (micropolar) parameter, $M = \frac{2\sigma_0 B_0^2}{\rho}$ indicates the magnetic field parameter, $Rd = \frac{16T_\infty^3\sigma^{\star}}{k^{*}\kappa}$ is the radiation parameter and $Gr = \frac{2xg\beta_T(T_w - T_\infty)}{U_0^2}$ is the Grashof number while $Pr = \frac{\mu cp}{\kappa}$ represents the Prandtl number. Also, the Eckert number is symbolized by $Ec = \frac{U_0^2}{\rho\,(T_w - T_\infty)}$ whereas $fw = -V_0\left(\frac{2}{U_0\nu}\right)^{\frac{1}{2}}$ denotes the suction/injection parameter with $V_0 = V_w x^{-\frac{1}{2}}$ being a constant, ($fw > 0$ suction , $fw < 0$ injection and $fw = 0$ means an impermeable sheet.

3.0 Results and Discussion

For the analysis of the results, we have made use of the following default values: $K = 5.0, Rd = 0.3\ \ Gr = 3.0,\ M = 1.0, n = 0.2, Q = Q^{*} = 0.2,\ \ Ec = 0.02,\ \ fw = 0.5, \varphi = 30°,\ \ Pr = 0.73$. The plots correspond to these values unless otherwise indicated on the graph. The nonnlinear differential equations (10-12) together with the boundary conditions (13) constitutes a two point boundary value problem (BVP) which are solved using shooting iteration technique alongside Runge-Kutta integration scheme. The quantities of engineering interest such as the skin friction coefficient Cf_x and the Nusselt number Nu_x (rate of heat transfer at the surface) are found out from the numerical computations. On setting $fw = Ec = n = Rd = 0$, the case of Rahman *et al.* (2009).is recovered. Table 1 shows the values of the skin friction coefficient and Nusselt number as compared with Rahman *et al.* (2009) for variation in the inclination angle parameter φ when $fw = Ec = n = Rd = 0$.
In the like manner, various values of magnetic parameter M for both Variable Electric Conductivity (VEC) and Constant Electric Conductivity (CEC) are found to be in good agreement as recorded in Tables 2. This confirms the correctness of the numerical code used in this work. Also, Tables 1 and 2, illustrate the reaction of Variable Electric Conductivity (VEC) and the Constant Electric Conductivity (CEC) on the skin friction coefficient Cf_x and the Nusselt number Nu_x for various values φ and M..

Table 1: Comparison of values of C_{fx} and Nu_x with Rahman *et al.* (2009) for variation in φ

	Rahman, *et al.* (2009)				Present Results			
φ	Cf_x VEC	Cf_x CEC	Nu_x VEC	Nu_x CEC	Cf_x VEC	Cf_x CEC	Nu_x VEC	Nu_x CEC
0°	4.2424	4.2932	0.6403	0.6536	4.2440	4.2922	0.6397	0.6531
30°	3.9488	3.9859	0.6139	0.6245	3.9507	3.9851	0.6132	0.6240
45°	3.5731	3.5942	0.5777	0.5848	3.5752	3.5936	0.5770	0.5842
60°	3.0215	3.0233	0.5188	0.5201	3.0242	3.0229	0.5178	0.5194

It is clearly revealed that the skin friction coefficient as well as the rate of heat transfer reduces with an increase in φ as seen in Table 1 whereas the values of skin friction coefficient as well the heat transfer Nu_x are higher for the case of Constant Electric Conductivity (CEC) than that of Variable Electric Conductivity (VEC). An increase in M has a decreasing effect on the skin friction coefficient Cf_x as well as on the rate of heat transfer at the surface for both cases of VEC and CEC.

Table 2: Comparison of values of C_{fx} and Nu_x with Rahman *et al.* (2009) for variation in M

	Rahman, *et al.*, (2009)				Present Results			
M	Cf_x VEC	Cf_x CEC	Nu_x VEC	Nu_x CEC	Cf_x VEC	Cf_x CEC	Nu_x VEC	Nu_x CEC
0	4.2427	4.2427	0.6841	0.6841	4.2395	4.2395	0.6820	0.6820
0.2	4.1950	4.2079	0.6740	0.6768	4.1931	4.2055	0.6222	0.6750
0.5	4.1352	4.1606	0.6607	0.6665	4.1348	4.1591	0.6593	0.6651
0.8	4.0859	4.1185	0.6493	0.6570	4.0864	4.1175	0.6480	0.6568
1.0	4.0574	4.0927	0.6424	0.6509	4.0583	4.0919	0.6412	0.6500
1.5	3.9973	4.0353	0.6270	0.6371	3.9988	4.0346	0.6262	0.6364
2.0	3.9488	3.9859	0.6139	0.6245	3.9507	3.9851	0.6132	0.6240

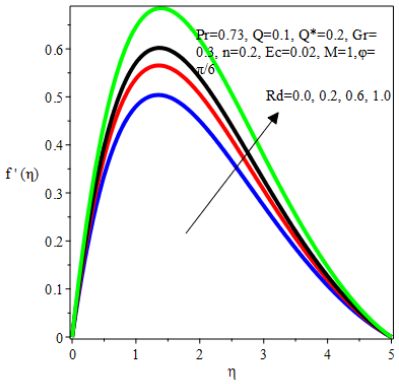

Figure 2 Velocity profiles for values of Rd

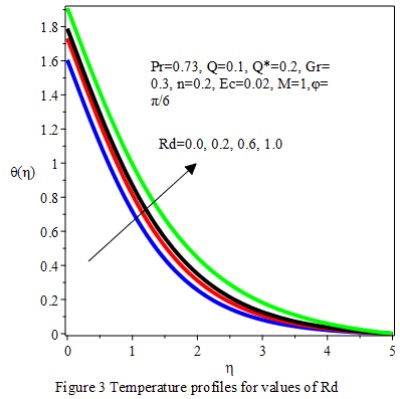

Figure 3 Temperature profiles for values of Rd

The plots of velocity and temperature profiles against η for various values of radiation parameter Rd are shown in Figures 2 and 3. It is evident that both velocity and temperature appreciate with an increase in Rd. The increase in temperature enhances heat transfer across the boundary layer (Figure 3) which in turn causes the fluid motion to ruse as seen in Figure 2. The rate of radiative heat transfer to the fluid increases and then causing the temperature of the fluid to rise. Hence, to have the cooling process at a faster rate, the radiation parameter Rd should be reduced.

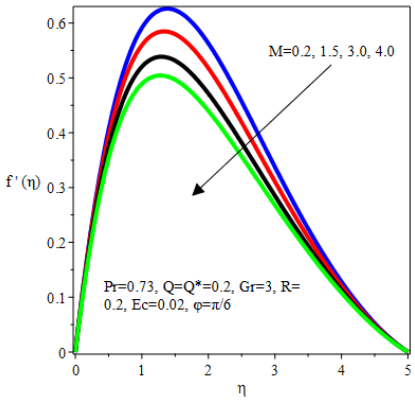

Figure 4 Velocity profiles for M

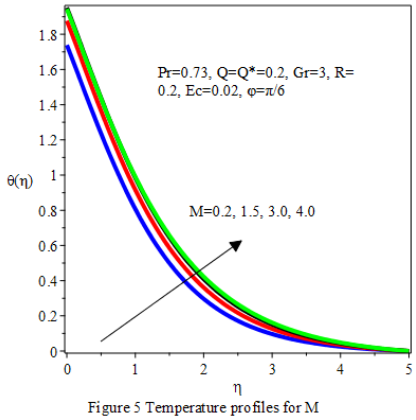

Figure 5 Temperature profiles for M

Figures 4-5 exhibit the impact of the magnetic parameter M on the velocity and temperature profiles respectively. It is noticed in Figures 4 that the velocity decreases with a rise in M due to the imposition of the Lorentz force which acts against the fluid motion. On the other hand, the temperature profiles rise with an increase in M Figure 5.

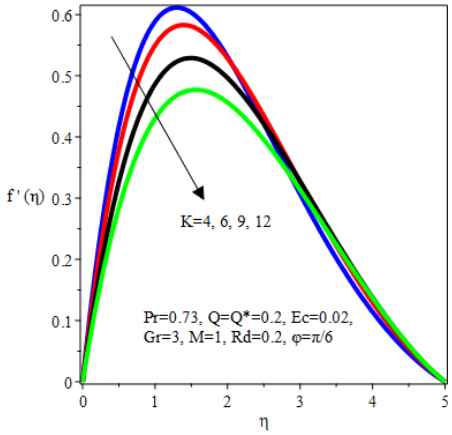

Figure 6 Velocity profiles for K

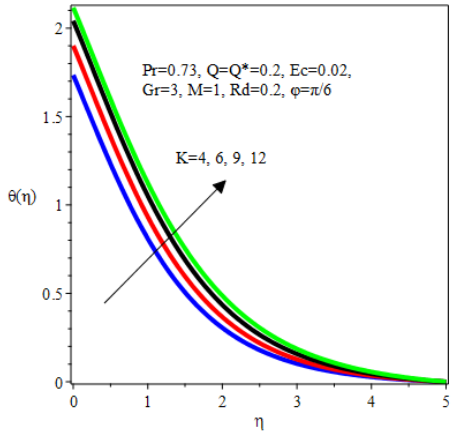

Figure 7 Temperature profiles for K

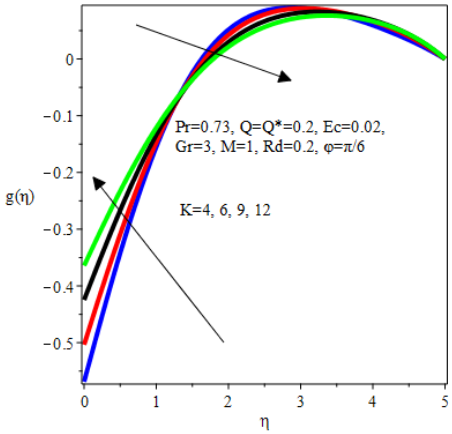

Figure 8 Microrotation profiles for K

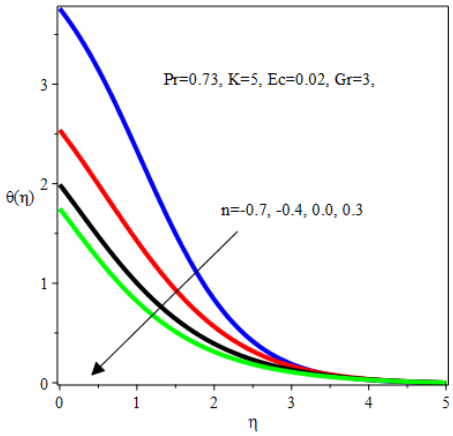

Figure 9 Temperature profiles for values of n

Figures 6-8 describe the effect of the micropolar parameter K on the velocity, temperature and microrotation respectively. The velocity diminishes with a rise in in the magnitude of K as seen in Figure 6 whereas the temperature accelerates with a rise in K as observed in Figure 7. The microrotation profiles rise near the sheet while further away from the sheet the profiles fall with a rise in K. The negative values denote the reverse rotation of the micro-particles. The impact of the surface temperature parameter n on the temperature profiles is displayed in Figure 9. It is observed that a rise the magnitude of n reduces the thermal boundary layer thickness which in turn lowers the average temperature across the boundary layer.

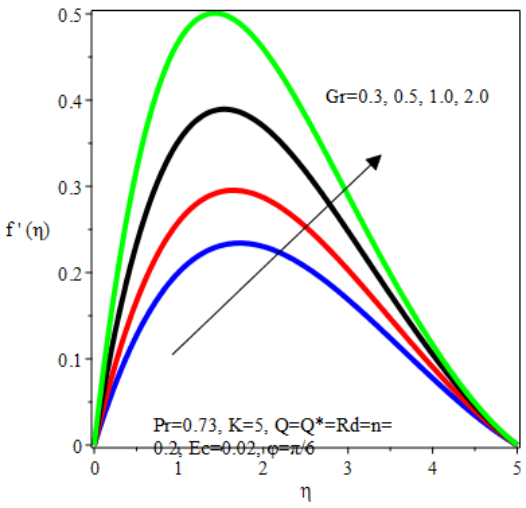

Figure 10 Velocity profiles for values of Gr

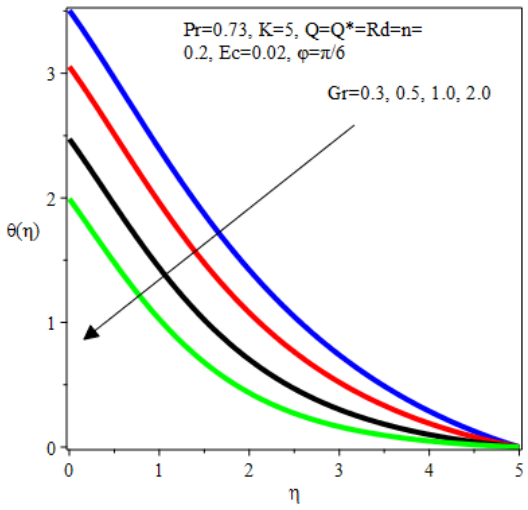

Figure 11 Temperature profiles for values of Gr

The influence of the Grashof number Gr on the velocity and temperature profiles are depicted in Figures 10 and 11. Evidently, the velocity profiles accelerate as the magnitude of Gr rises as shown in Figure 10. Physically, Gr indicates the relative effect of the thermal buoyancy force to the viscous hydrodynamic force in the boundary layer. Hence, a rise in Gr enhances buoyancy forces which acts as a favourable pressure gradient accelerating the fluid within the boundary layer. Contrarily, the temperature profiles fall as the magnitude of Gr increases as displayed in Figure 11.

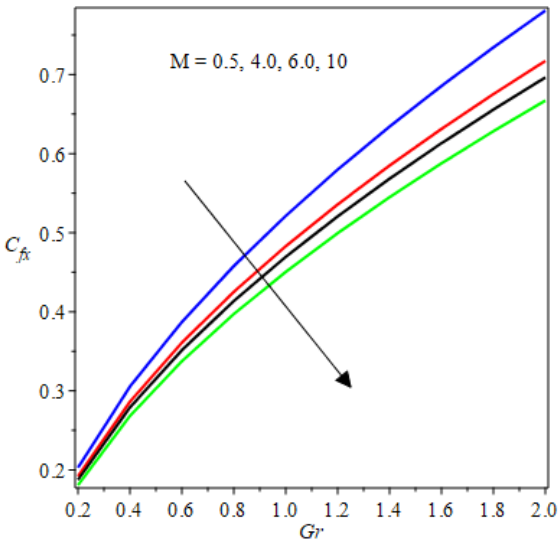

Figure 12 Effects of Gr and M on Cfx

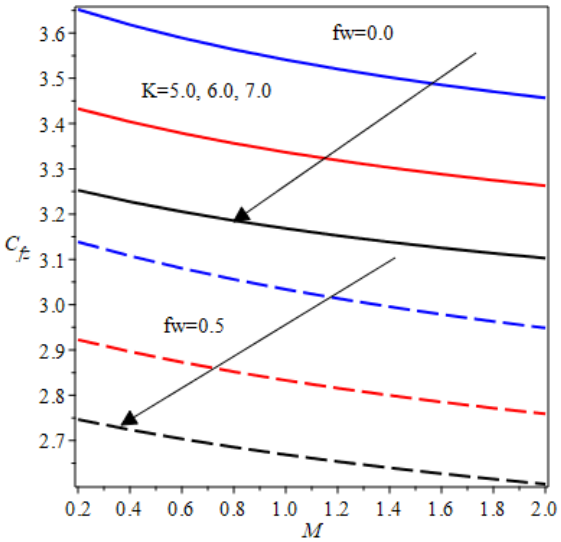

Figure 13. Effects of M & K on Cfx

Figure 12 illustrates the influence of both Grashof number and magnetic field parameter on the skin friction coefficient C_{fx} An increase in M produces a damping effect on the skin friction C_{fx} coefficient whereas the skin friction coefficient rises with an increase in Gr for a fixed value of M as shown in Figure 12.
Figure 13 is a plot of the skin friction coefficient C_{fx} against the magnetic field parameter M for various values of the micropolar parameyбer K when the sheet is permeable $(fw = 0.50)$ and impermeable $(fw = 0)$. The shear stress at the surface C_{fx} decreases with increase in both M and K, however, the shear stress reduces better with permeable sheet than that of impermeable sheet as seen in Figure 13.

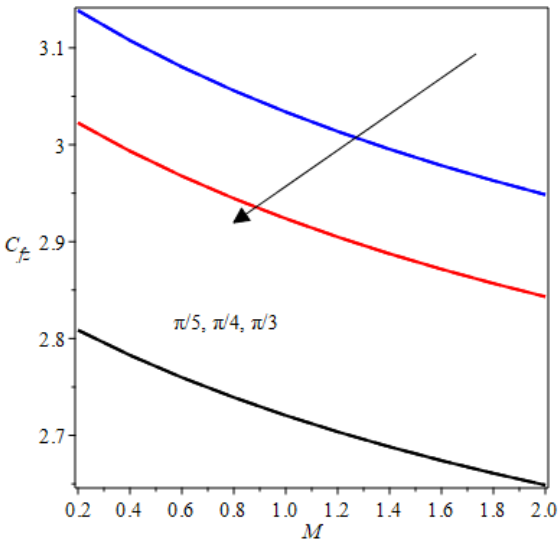

Figure 14. Effect of M & φ on Cfx

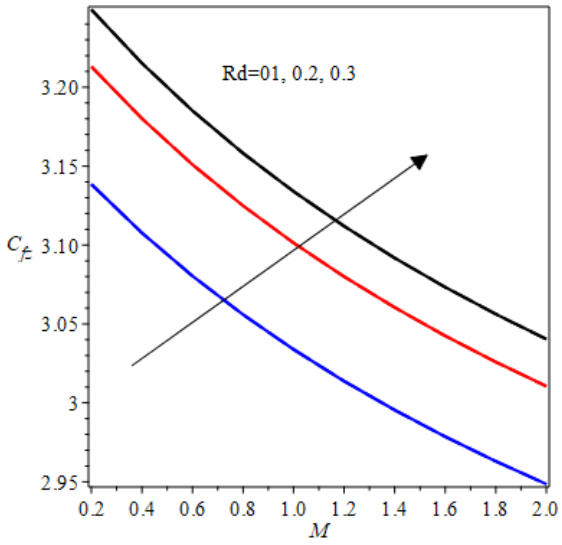

Figure 15. Effects of Rd & M on Cfx

Figure 14 shows the impact of the angle of inclination φ on the skin friction coefficient. It is noticed that there is a reduction in the skin friction coefficient C_{fx} with an increase in φ for fixed value of M. Hence φ tends to reduce C_{fx} On the contrary, the graph of the shear stress at the surface C_{fx} versus the magnetic field parameter M for variation in the radiation parameter Rd shows that an increase in the radiation parameter Rd enhances the skin friction coefficient for any value of the magnetic field parameter M.

Conclusion

The analysis of thermal radiation effect on hydromagnetic flow and heat transfer of micropolar fluid with the influence of Joule heating, and variable electrical conductivity has been investigated in this study. The thermal boundary condition has been assumed to be variable heat flux while the heat source/sink is taken to be non-uniform. The set of governing equations has been transmuted from partial to ordinary differential equations and then solved numerically via shooting technique alongside fourth order Runge-Kutta integration scheme. The influences of the main controlling parameters have been analyzed with graphs.
Summarily, the following points are deduced from the study:

- The viscous drag at the surface can be reduced by using the non-Newtonian micropolar fluid as a working fluid during fabrication processes. This helps to reduce the friction better than the Newtonian fluids.
- The imposition of magnetic field parameter reduces the friction on the skin of the sheet, hence, magnetic field parameter can be used to reduce the viscous drag along the surface.

- The temperature distribution across the boundary layer diminishes with an increase in the surface temperature and thermal buoyancy parameters. However, the skin friction coefficient rises with thermal buoyancy parameter.
- The velocity and temperature of the micropolar fluid accelerate as the radiation parameter increases. Hence, to have cooling at a faster rate, the radiation should be minimized.

REFERENCES

Ahmadi, G. (1976). Self-similar solution of incompressible micropolar boundary layer flow over a semi-infinite plate, *Int. J. Engng Sci*, **14**, 639-646.

Ariman, T., Turk, M. A. and Sylvester, N. D. (1973). Micro continuum fluid mechanics - A review, *Int. J. Engng Sci*, **11**, 905-930.

Chen, J., Liang, C. and Lee J. D. (2011). Theory and simulation of micropolar fluid dynamics, J. Nanoengineering and nanosystems, **224**: 31-39.

Cortell, R. (2008). Effects of viscous dissipation and radiation on the thermal boundary layer on nonlinearly stretching sheet, *Physics Letters A*, **372,** 631-636.

Crane, L. J. (1970). Flow past a stretching plate, *Communicatios Breves*, **21**, 645-647.

Darbhashayanam, S. and Mendu, U.(2014). Thermal radiation and chemical reaction effects on magnetohydrodynamic free convection heat and mass transfer in a micropolar fluid, *Turkish Journal of Engineering and Environmental Sciences*, **38**, 184-196.

Eringen, A. C. (1964). Simple microfluids., *International Journal of Engineering Science, **2***(2), 205-217.

Eringen, A. C. (1966). Theory of micropolar fluids, J. Math. Anal. Appl., **16**: 1-18.

Eringen, A. C. (1972). Theory of thermo-microfluids, Journal of Mathematical Analysis and Applications, **38**: 480-496.

Fatunmbi, E. O and Fenuga, O. J. (2017). MHD micropolar fluid flow over a permeable stretching sheet in the presence of variable viscosity and thermal conductivity with Soret and Dufour effects, *International Journal of Mathematical Analysis and Optimization: Theory and Applications*, **2017**: 211- 232.

Fatunmbi, E. O. and Adeniyan, A. (2018). MHD stagnation point-flow of micropolar fluids past a permeable stretching plate in porous media with thermal radiation, chemical reaction and viscous dissipation, *Journal of Advances in Mathematics and Computer Science*, **26**: 1-19.

Gupta, P. S. and Gupta, A. S. (1977). Heat and mass transfer on a stretching sheet with suction or blowing. {\it Can. *J. Chem. Eng.*, **55**, 744-746.

Hayat, T., Shehzad, S. A. and Qasim, M. (2011). Mixed convection flow of a micropolar fluid with radiation and chemical reaction, *Int J. Numer Meth*, **67**:1418-1436.

Helmy, K. A. (1995). MHD boundary layer equations for power-law fluids with variable electric conductivity, *Meccanica*, **30**, 187-200.

Ibrahim, S. M. (2014). Effects of chemical reaction on dissipative radiative MHD flow through a porous medium over a nonisothermal stretching sheet. J*ournal of Industrial Mathematics*, 1-10. doi.org/10.1155/2014/243148.

Jena, S. K. and Mathur, M. N. Similarity solutions for laminar free convection flow of a thermomicropolar fluid past a non-isothermal flat plate, *Int. J. Eng. Sci.* **19**, 1431-1439.

Kumar, L. (2009). Finite element analysis of combined heat and mass transfer in hydromagnetic micropolar flow along a stretching sheet, *Computational Materials science*, **46**, 841-848.

Lukaszewicz, G. *Micropolar fluids: Theory and Applications*, 1st Ed., Birkhauser, Boston, 1999.

Mahmoud, M. A. A. (2011). Hydrodynamic stagnation point flow towards a porous stretching sheet with variable surface heat flux in the presence of heat generation, *Chem. Eng. Comm*., **198**, 837-846.

Mohamed, R. A. and Abo-Dahab, S. M. (2009). Influence of chemical reaction and thermal radiation on the heat and mass transfer in MHD micropolar flow over a vertical moving porous plate in a porous medium with heat generation, *International Journal of Thermal Sciences*, **48** 1800-1813.

Mukhopadhyay, S. (2013). Slip effects on MHD boundary layer flow over an exponentially stretching sheet with suction/blowing and thermal radiation, *Ain Shams Engineering Journal*, **2013,** 485-491.

Olanrewaju, P. O., Okedayo, G. T. and Gbadeyan, J. A. (2011). Effects of Thermal Radiation on MH Flow of a Micropolar Fluid towards a Stagnation Point on a Vertical plate, *International Journal of Applied Science and Technology*, **1**(6), 1-12.

Pal, D. and Chatterjee, S. (2010). Heat and mass transfer in MHD non-Darcian flow of a micropolar fluid over a stretching sheet embedded in a porous media with non-uniform heat source and thermal radiation, *Commun Nonlinear Sci. Numer Simulat*, **15**, 1843-1857.

Peddieson, J and McNitt, R. P. (1970). Boundary layer theory for micropolar fluid, *Recent Adv. Enggng Sci*., **5**, 405.

Peddieson, J. (1972). An application of the micropolar model to the calculation of a turbulent shear flow, *Int. J. Eng. Sci*., **10:** 23-32.

Rahman, M. M., 2009. Convective flows of micropolar fluids from radiate isothermal porous surface with viscous dissipation and joule heating, *Commun Nonlinear Sci. Numer Simulat,14*, 3018-

Reddy, M. G. (2012). Heat generation and thermal radiation effects over a stretching sheet in a micropolar fluid, *International Scholarly Research Networks,* **2012**: 1-6. doi.org. /10.5402/2012/795814.